Direct Vortex Lattice Imaging and Tunneling Spectroscopy of Flux Lines on $YBa_2Cu_3O_{7-\delta}$

I. Maggio-Aprile, Ch. Renner, A. Erb, E. Walker, and Ø. Fischer

Département de Physique de la Matière Condensée, Université de Genève, 24, Quai E.-Ansermet, CH-1211 Genève 4, Switzerland

(Received 5 July 1995)

We report the observation of the flux line lattice in $YBa_2Cu_3O_{7-\delta}$ by scanning tunneling microscopy. The measurements were carried out at 4.2 K and in a magnetic field of 6 T applied along the c axis. The vortices appear arranged in an oblique lattice in which the primitive vectors are nearly equal and form an angle of approximately 77°. We also report local tunneling spectroscopy into a vortex core which reveals two peaks separated by about 11 meV. The zero-field spectra are reproducible over large areas of the sample and show a multiple peak structure.

PACS numbers: 74.60.Ge, 71.20.Cf, 74.50.+r, 74.72.Bk

There is a continuing large effort devoted to investigate the vortex phases in high temperature superconductors (HTS's). In the past, scanning tunneling spectroscopy (STS) was successfully applied to investigate the vortex lattice 2H-$NbSe_2$ and 2H-$Nb_{1-x}Ta_xSe_2$ [1,2]. This technique probes the quasiparticle local density of states (LDOS) and thus indirectly the order parameter. Since these quantities vary on the scale of the coherence length ξ, this technique can in principle probe the whole H-T diagram of the superconductor. Other real space imaging techniques such as the decoration technique [3] and magnetic force microscopy [4] use the magnetic field variations due to the vortex lattice and are thus inherently limited to relatively low fields because of the large penetration depths in the HTS. Furthermore, the STS experiments demonstrated the unprecedented capabilities of scanning tunneling microscopy (STM) in probing the electronic structure of the vortex core. Thus, it is of considerable interest to be able to use this technique also on HTS's. In particular, the study of the local quasiparticle excitation spectrum of a single flux line predicted by Caroli, de Gennes, and Matricon [5] constitutes a considerable challenge. In the STM investigations on $NbSe_2$ and $Nb_{1-x}Ta_xSe_2$, these states could not be resolved, by they appeared as a zero bias anomaly in the tunneling spectra at the center of the flux line. In HTS's the energy spacing is expected to be within the energy resolution of tunneling spectroscopy. Such experiments may allow a direct probe of fundamental properties of HTS's such as the superconducting gap (Δ), the coherence length (ξ), the Fermi energy (E_F), and the pairing symmetry. Hence, STS applied to the mixed state in HTS's holds promise to shed new light on the fundamental nature of high temperature superconductivity.

However, there is a basic difficulty in completing this kind of experiment due to its stringent requirements for very reproducible tunneling conditions. We have recently demonstrated such reproducible vacuum STS on cleaved surfaces of $Bi_2Sr_2CaCu_2O_{8-\delta}$ (BSCCO) [6,7]. However, to date we have not been able to observe the expected signatures of the vortex cores on this compound. Possible reasons for this will be discussed below. We therefore turned to $YBa_2Cu_3O_{7-\delta}$ (YBCO). Many groups have reported tunneling on this compound [8,9], but no consensus about the intrinsic tunneling spectra has emerged. A possible reason for this is that YBCO tends to have an insulating surface resulting from a (dead) topmost layer and, therefore, it has become very difficult to perform tunneling spectroscopy with an ideal barrier. We have been able to overcome these difficulties partly by improving the electrical and mechanical noise level of our STS experimental setup in high fields and partly by using single crystals of improved surface quality. In this Letter we report the first imaging of the vortex lattice by STS on a HTS. These real space images of the flux line lattice allow us to precisely position the tip within the vortex core and measure for the first time the LDOS of individual flux lines on a HTS.

The tunneling experiments presented here were performed on a fully oxygenated YBCO twinned single crystal [10]. The crystal, having an inductively measured T_c of 91 K, was grown in the recently discovered crucible material $BaZrO_3$. This material has the advantage that it does not react with the highly reactive melts used as solvents for YBCO. Because of this fact, crystals out of such growth experiments are not contaminated with impurities from the container material and high purity can be obtained using high quality starting materials (purity 99.999 at. %, Cerac, Milwaukee). Detailed conditions for the crystal growth are given elsewhere [10]. No particular surface conditioning was done prior to the tunneling experiments. We used chemically etched pure iridium tips. Our experimental setup is described in detail elsewhere [11]. The acquisition of the tunneling spectra was carried out in a standard way. We measured the tunneling current $[I(V)]$ at constant tip-sample spacing (opened feedback loop) while the bias voltage was swept over a specific energy range. The differential conductance spectra $[dI/dV(V)]$ were extracted using a lock-in amplifier with a typical ac modulation in the range 0.5–1.0 mV. Between spectra, typical tunneling parameters are $I = 0.5$ nA and $V = 0.5$ V giving a tunneling

 0031-9007/95/75(14)/2754(4)$06.00

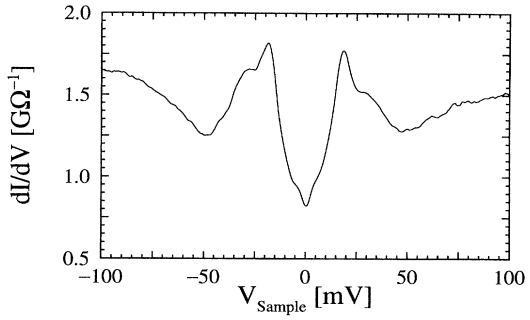

FIG. 1. Differential conductance spectrum $dI/dV(V)$ of an YBCO crystal at $T = 4.2$ K, $H = 0$ T.

resistance as high as 1 GΩ. This was necessary in order to ensure vacuum tunneling conditions, as defined in Ref. [7], implying a sufficiently large tip-sample distance. The topography of the surface shows terraces of $(1-5)\times10^4$ nm^2 with a roughness of about 0.1 nm. The zero-field spectra were uniform over a plateau, but some plateaus showed an insulating behavior.

A characteristic superconductor–insulator–normal metal differential conductance spectrum obtained on an YBCO single crystal at 4.2 K is shown in Fig. 1. We observe three gaplike features. The main one corresponds to a conductance peak close to 20 ± 2 meV. Slightly beyond this feature, a second conductance peak, which is usually less developed than the former, appears in the 25 to 30 meV range. A third gaplike feature appears at low bias. However, this one is weaker and less reproducible, and its conductance peaks vary in energy (4 to 10 meV), as well as in amplitude. The background conductance beyond these gaplike features always increases linearly with increasing bias. Therefore we are not able to say from these measurements whether or not the asymmetric dip observed earlier in the spectra of BSCCO [7] is also present here. The zero-bias conductance (ZBC) amounts in all our measurements to about 60%–70% of the normal state conductance defined at approximately 50 meV. This is much higher than the ZBC measured on BSCCO single crystals [6,7]. The question of course arises as to how well these spectra reflect the intrinsic quasiparticle density of states. We first emphasize that these structures are stable against changes in the tip-sample spacing and that they are reproducible while scanning the tip over several hundred Å along the sample surface in the Meissner state. We also observe systematically the same type of spectra over much larger areas of the sample. Although variations in the peak intensities occur, all features seen in Fig. 1 are systematically present. We also note the remarkable similarities of this local probe spectrum with the planar junction data obtained by Valles *et al.* [9], with respect to both the peak structure as well as the zero bias conductance. The fact that such different techniques yield similar tunneling spectra further strengthens our feeling that the features we are probing are relevant to the superconducting LDOS in YBCO.

The spectrum shown in Fig. 1 is clearly not consistent with an isotropic BCS *s*-wave picture. Also, it is very different from the simple *d*-wave picture, which is close to, but not identical to the spectra observed on BSCCO [7]. The multiple peak structure more resembles the spectrum expected for an extended *s* wave [12] except for the large zero-bias conductivity. In any case these results reveal a complex behavior of the order parameter. The presence of the chains in the crystal structure of YBCO may be partly responsible for the difference between YBCO and BSCCO [13]. However, since the relative strength of the peaks does not vary appreciably with tip-sample distance, it appears unlikely that the different peaks correspond to gaps in different layers.

We now turn to the systematics of the conductance spectra measured with a magnetic field applied perpendicular to the YBCO basal *a-b* plane. When the tip is positioned outside the vortex cores, the conductance spectra are basically identical to those measured in the Meissner state (Fig. 1). On the other hand, we measure completely different tunneling spectra when the tip enters the core region of a flux line. The fact that these differences are due to the presence of a vortex core beneath the tip is asserted by the possibility to obtain an image of the flux line lattice by mapping these systematic changes in real space. Figure 2(a) shows such a map over a 100 nm ×100 nm area at 4.2 K and 6 T (field cooled), where we used the ratio of the conductance peak at 20 meV to the ZBC to define a grey scale as a function of position [2]. The dark regions in Fig. 2(a) correspond to the vortex cores, where the ZBC is increased with respect to the conductance at 20 meV. The vortices are arranged in an oblique lattice. The primitive vectors are approximately equal and the angle between them is found to be 77° ± 5°. This is in good agreement with recent small angle neutron scattering studies [14]. However, the lattice appears disordered

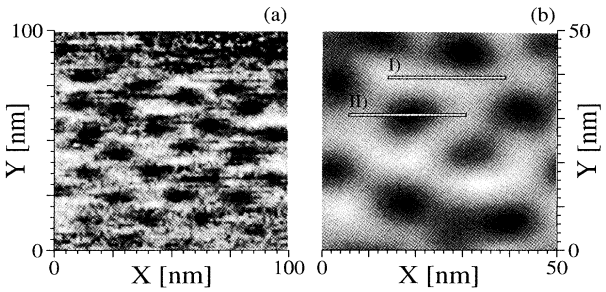

FIG. 2. Spectroscopic images of the vortex lattice acquired on an YBCO crystal at $T = 4.2$ T, $H = 6$ T. (a) 100 × 100 nm^2 scan-area, raw data. (b) 50 × 50 nm^2 scan-area, filtered data. The lines I and II correspond to the paths used to acquire Figs. 3(a) and 3(b), respectively.

without long range order, reflecting more a vortex glass state than a regular lattice. The density of vortices corresponds to a local field slightly higher then 6 T. After reducing the external field to zero a few vortices remain in the image. We have verified that in zero field the STS image is uniform without vortices.

We observe an elongated shape of the vortex cores. In Fig. 2(b) we show a Wiener filtered vortex map in order to better identify this elongation. The ratio of the axes in the apparent elliptic shape is about 1.5. The large axis, referred to as the x direction, is either in the a or in the b direction of the crystal. Since the crystal was twinned and we do not yet have atomic resolution we cannot distinguish between a and b. We have verified that this elongation is independent of the scanning direction of the tip. We have also found other areas on the surface where the elongation was in the perpendicular direction, probably corresponding to a twin domain with inverted a and b axes. This elongation either reflects fluctuations in the position of the vortex line or it reflects a true a-b anisotropy. Within the former hypothesis we would have to conclude on a preferential direction (either a or b) for the fluctuations. However, if this elongation reflects an intrinsic a-b plane anisotropy, the ratio of the coherence lengths in the a and b directions would be $\xi_a/\xi_b \approx 0.67$ (or 1.5 since we cannot presently distinguish a and b). This anisotropy would be in agreement with recently reported a-b anisotropies for λ ($\lambda_a/\lambda_b \approx 1.5$) [15]. Such an anisotropy would lead to a distorted hexagonal lattice, compressed in the y direction with an angle of 98° between the primitive vectors of the oblique unit cell, in clear contrast to the observed value of 77°. Thus the observed lattice must in addition be influenced by the local symmetry of the vortex cores. This could come from crystal field effects of the orthorhombic lattice or it could reflect the order parameter symmetry. Note that this observation is in apparent disagreement with earlier Bitter decoration technique experiments on YBCO [3]. These measurements carried out at much lower magnetic fields show a nearly hexagonal Abrikosov lattice. However, at higher fields, the distance between the cores becomes small, and competition between electrodynamical effects and spatial variations of the superconducting order parameter near the vortex core might take place. Note that since our sample was twinned we cannot at this point exclude that this influenced either the distorted lattice or its disordered nature.

Differential conductance spectra were acquired along two 25 nm paths in the x direction at 4.2 K in a magnetic field of 6 T [paths are shown in Fig. 2(b) as I and II]. One of these lines was in between vortices (a) and the other across a flux line (b). The spectra, shown in Fig. 3, were acquired every 1 nm along these lines. Away from the cores (a), the spectra are the same along the whole line, and they are similar to those measured in zero field. In the other case (b), the spectra evolve while approaching the

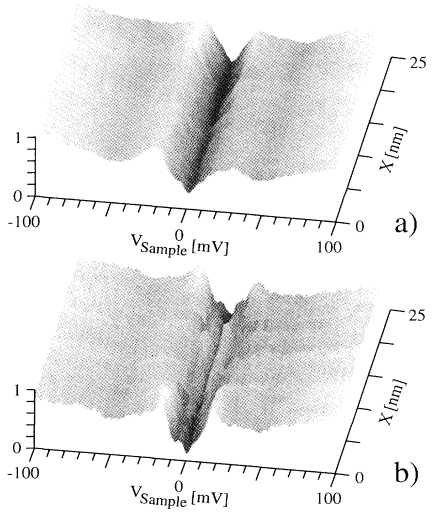

FIG. 3. Differential conductance spectra measured as a function of position on an YBCO crystal ($T = 4.2$ K, $H = 6$ T). The paths are 25 nm long [see Fig. 2(b), lines I and II]. (a) Between vortex cores, (b) across a vortex core.

core center. First the 20 meV conductance peak decreases in magnitude and totally disappears at the middle of the core. At the same time, the 27 meV peak does not vanish completely and a broad bump, although often reduced, remains. The most striking feature is the low energy peaks which develop inside the core. Figure 4 shows the average spectrum obtained from a scan over 5 nm across a vortex core. It has two low bias conductance peaks separated by 11 meV. Many studies have focused on the quasiparticle LDOS inside a vortex core [5,16]. The pair potential $\Delta(r)$ inside the core leads to bound states at energies $E_\mu = \pm 2\mu K\Delta^2/E_F$ ($\mu = \frac{1}{2}, \frac{3}{2}, \frac{5}{2}, \ldots$; and K is of order of unity). We tentatively identify the two peaks with the first two levels $E_{1/2} = \pm K\Delta^2/2E_F$. Taking $\Delta = 20$ meV from our spectra, we find $E_F/K = 72$ meV. This gives a ratio $E_F/K\Delta = 3.6$. Recent infrared absorption experiments found 9.5 meV for the lowest quasiparticle pair creation energy [17]. This value is in good agreement with our data.

As the tip moves away from the vortex center it is expected that the next localized states should show up in the spectra [16]. Assuming constant energy level spacing, the second localized state ($\mu = +3/2$) is expected at $E_{3/2} = 16.5$ meV. In Fig. 3(a), no peak is seen throughout the line at this energy. However, the conductance peak which develops at 20 meV with increasing distance from the vortex core may obscure the contribution of the $E_{3/2}$ state. In any case, the high value of $E_{1/2}$ with respect to Δ is indicating that very few quasiparticle states can exist inside an YBCO vortex core, namely, 2 ($\mu = \pm\frac{1}{2}$)

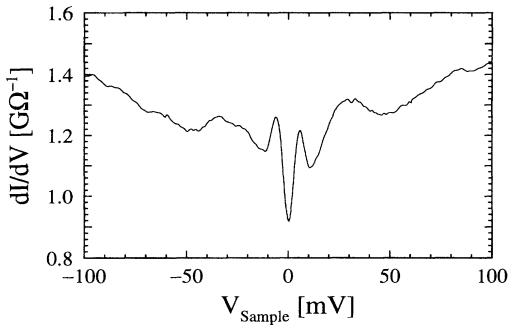

FIG. 4. Average spectrum calculated from conductance measurements performed at the center of a vortex core, along a 5 nm path (YBCO crystal, $T = 4.2$ K, $H = 6$ T).

or 4 ($\mu = \pm\frac{1}{2}, \pm\frac{3}{2}$) (any higher level excitation would lie at $E > \Delta$). Thus the vortex cores are in an extreme quantum limit. One point that remains open and needs further investigation is the possible relation between the weak low energy anomalies in zero field ($\approx$5 meV) and the much stronger peak structures at approximately the same energy in the vortex cores, as well as the remnant of the 27 meV structure in the vortex cores. Note that the expected magnetic field dependent shifts of the localized states are estimated to be less than 1 meV and thus too small to be seen in our present data.

Let us finally comment on the difficulties we have encountered in trying to observe the vortex lattice in BSCCO. One possible reason may arise from the highly anisotropic nature of HTS's, which renders vortex motion possible, even at 4.2 K. This problem could be particularly perturbing in BSCCO, which is very anisotropic. YBCO, on the other hand, is much less anisotropic and we expect these efforts to be much less severe. In fact, the position of the vortices remained remarkably stable for period of several days. Another possible explanation could be that the larger gap in BSCCO as compared to YBCO pushes the first states $E_{\pm 1/2}$ beyond the superconducting gap which would imply that no localized states would be present in the vortices in BSCCO. This question clearly needs further investigation.

In conclusion, we have successfully probed the superconducting spectra on YBCO crystals, at 4.2 K and we find a non-BCS-like spectrum similar to those reported for planar junctions. We also report the first vortex lattice imaging by STS on a HTS and we have demonstrated the capability of this method to work at high magnetic fields. This study reveals a locally oblique lattice with no apparent long range order at the field and temperature we studied. We also report the first study of the LDOS of a vortex core. We tentatively identify the two peaks in the LDOS as the signature of the first two localized states $E_{\pm 1/2}$ ($\pm$5.5 meV).

We are grateful to A. Takagi who shared his experience in etching pure iridium wires. We have benefited from the technical assistance of J.-G. Bosch and L. Hoffman. We thank R. Flukiger for his support towards the improved crystal growth. This work was supported by the Swiss National Science Foundation.

[1] H. F. Hess, R. B. Robinson, R. C. Dynes, J. M. Valles, Jr., and J. V. Waszezak, Phys. Rev. Lett. **62**, 214 (1989).
[2] Ch. Renner, A. D. Kent, Ph. Niedermann, Ø. Fischer, and F. Lévy, Phys. Rev. Lett. **67**, 1650 (1991).
[3] G. J. Dolan *et al.*, Phys. Rev. Lett. **62**, 2184 (1989); L. Vinnikov *et al.*, Zh. Eksp. Teor. Fiz. **49**, 83 (1989).
[4] A. Moser *et al.*, Phys. Rev. Lett. **74**, 1847 (1995); P. Rice and J. Moreland, IEEE Trans. Magn. **27**, 5181 (1991).
[5] C. Caroli, P. G. de Gennes, and J. Matricon, Phys. Lett. **9**, 307 (1964); C. Caroli, Ann. Inst. Henri Poincaré A **4**, 159 ().
[6] Ch. Renner, Ø. Fischer, A. D. Kent, D. B. Mitzi, and A. Kapitulnik, Physica (Amsterdam) **194–196B**, 1689 (1994).
[7] Ch. Renner and Ø. Fischer, Phys. Rev. B **51**, 9208 (1995).
[8] H. L. Edwards *et al.*, Phys. Rev. Lett. **69**, 2967 (1992); T. G. Miller *et al.*, Phys. Rev. B **48**, 7499 (1993); M. Nantoh *et al.*, J. Appl. Phys. **75**, 5227 (1994).
[9] J. M. Valles, Jr., R. C. Dynes, A. M. Cucolo, M. Gurvitch, L. F. Schneemeyer, J. P. Garno, and J. V. Waszczak, Phys. Rev. B **44**, 11 986 (1991).
[10] A. Erb, E. Walker, and R. Flükiger, Physica (Amsterdam) **245C**, 245 (1995); A. Erb, Ph.D. thesis, Universitat Karlsruhe, Germany, 1994.
[11] Ch. Renner *et al.*, J. Vac. Sci. Technol. A **8**, 330 (1990); A. D. Kent *et al.*, Ultramicroscopy **42–44**, 1631 (1992).
[12] For discussion of possible pairing states, see D. J. Scalapino, Phys. Rep. **250**, 329 (1995).
[13] M. Tachiki, S. Takahaski, F. Steglich, and H. Adrian, Z. Phys. B **80**, 161 (1990).
[14] B. Keimer, W. Y. Shih, R. W. Erwin, J. W. Lynn, R. Dogan, and I. A. Aksay, Phys. Rev. Lett. **73**, 3459 (1994).
[15] K. Zhang, D. A. Bonn, S. Kamal, R. Liang, D. J. Baar, W. N. Hardy, D. Basov, and T. Timusk, Phys. Rev. Lett. **73**, 2484 (1994).
[16] F. Gygi and M. Schluter, Phys. Rev. B **43**, 7609 (1991).
[17] K. Karrai, E. J. Choi, F. Dunmore, S. Liu, H. D. Drew, Q. L. Li, D. B. Fenner, Y. D. Zhu, and F. C. Zhang, Phys. Rev. Lett. **69**, 152 (1992).

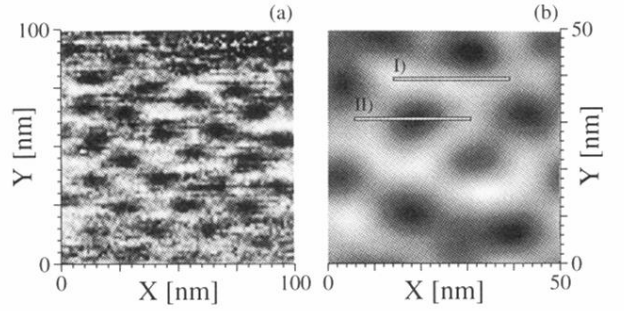

FIG. 2. Spectroscopic images of the vortex lattice acquired on an YBCO crystal at $T = 4.2$ T, $H = 6$ T. (a) 100×100 nm^2 scan-area, raw data. (b) 50×50 nm^2 scan-area, filtered data. The lines I and II correspond to the paths used to acquire Figs. 3(a) and 3(b), respectively.

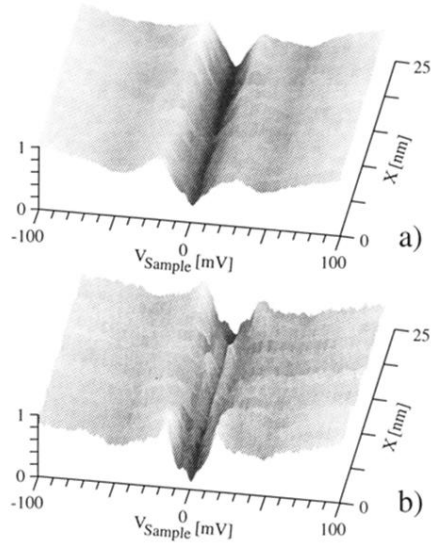

FIG. 3. Differential conductance spectra measured as a function of position on an YBCO crystal ($T = 4.2$ K, $H = 6$ T). The paths are 25 nm long [see Fig. 2(b), lines I and II]. (a) Between vortex cores, (b) across a vortex core.